

Synthesis of MCM-41 from coal fly ash by a green approach: Influence of synthesis pH

K.S. Hui, C.Y.H. Chao*

Department of Mechanical Engineering, The Hong Kong University of Science and Technology, Clear Water Bay, Kowloon, Hong Kong, China

Received 13 July 2005; received in revised form 27 February 2006; accepted 26 March 2006

Available online 25 April 2006

Abstract

The present study reports a green synthesis method for preparing pure (free of fly ash) and ordered MCM-41 materials from coal fly ash at room temperature (25 °C) during 24 h of reaction. It was shown that the impurities in the coal fly ash were not detrimental to the formation of MCM-41 at the tested conditions. The influence of initial synthesis pH on material properties of calcined MCM-41 samples was investigated by various techniques such as XRF, XPS, XRD, FTIR, DR–UV–vis, solid state NMR, N₂ physisorption, TG-DTA, SEM and TEM. The experimental results showed that the amount of trace elements such as Al, Na, Ti and Fe incorporated into the sample increased with synthesis pH value. More aluminum species were incorporated with tetrahedral coordination in the framework under a high pH value. The particle size of the sample decreased with the synthesis pH value. Samples synthesized at high pH values had a larger pore size and were more hydrothermally stable than those at low pH values. From thermal analysis, it was observed that the synthesized MCM-41 samples showed a high thermal stability. These properties made the synthesized MCM-41 suitable for further processing into more useful materials in a wide range of applications.

© 2006 Elsevier B.V. All rights reserved.

Keywords: Coal fly ash; MCM-41; Synthesis; Green; Recycle

1. Introduction

Since scientists at Mobil Oil Research and Development announced the successful synthesis of mesoporous molecular sieves (M41S) in 1992 [1–3], numerous studies on their synthesis, characterization and application have been reported [4,5]. A typical synthesis starts with the formation of organic micellar species in an aqueous solution, followed by the polycondensation of an inorganic matrix, and ends with the removal of the organic template [6]. Interaction between the organic surfactant and the inorganic matrix is dictated by the synthesis reagents and the preparation conditions is a controlling factor in influencing the physical and chemical properties of the synthesized mesoporous materials [7,8]. Mesoporous materials with pore sizes ranging from 2 to 50 nm have found a lot of applications in shape-selective catalysis [9], adsorption of gases and liquid [10–13], biomolecular immobilization [14] and separation [15] because of their high specific areas and large uni-

form pore sizes. MCM-41, consisting of hexagonal arrays of a uniform pore size, is a member of M41S and has attracted extensive attention of researchers in academia and industry because of its large pore, large surface area, thermal stability and mild acidic property. The incorporation of different elements within the silica framework of MCM-41 has been implemented in order to increase the acidity, ion exchange capacity and specific catalytic activity of the mesoporous silica molecular sieves [16–22].

Generally, templates used for synthesis of M41S are selected from the alkyl trialkyl ammonium halide surfactant family. The source of silica for the synthesis could be either costly organic silica precursors such as silicon alkoxides or cost efficient substances like sodium silicate. The high cost of synthesizing M41S materials is mainly due to the high cost of templates. Recently, Dai et al. [23] used ethyl acetate (CH₃COOC₂H₅) as a mild acid hydrolyser in the synthesis of MCM-41 materials under environmentally friendly conditions where no toxic waste was generated. Using cheap inorganic silica sources [24] instead of expensive ones as well as a mild acid hydrolyser in the synthesis can be an important improvement to the industrial scale production of M41S materials.

* Corresponding author. Tel.: +852 2358 7210; fax: +852 2358 1543.
E-mail address: meyhchao@ust.hk (C.Y.H. Chao).

Coal fly ash is the waste product of coal combustion in a coal-fired power station. Large quantities of coal fly ash are produced in electric power plants throughout the world every year. The amount of coal fly ash formed is approximately 500 million tonnes per year and is predicted to increase. The global recycling rate of fly ash is only 15% [25]. Coal fly ash contains a certain amount of metal oxides which will inevitably be released to the environment if it is not converted into useful materials. Efficient disposal of coal fly ash is a worldwide issue because of the huge amount produced and its harmful effects on the environment [26–28]. At present, resource recovery from coal fly ash is one of the most important issues in waste management [25,29,30]. Converting coal fly ash into useful materials may have important economic and environmental implications. For example, reuses of coal fly ash may provide a new source of revenue for the power production companies and eliminate previous expenses associated with its disposal. A detailed cost analysis on the feasibility of recycling coal fly ash can be obtained in our previous work [31]. In the environmental aspect, the increased use of coal fly ash can reduce the need for additional landfill space and conserve natural resources. For example, a tonne of coal fly ash, compressed to 70 pounds per cubic foot, normally takes up approximately 28 cubic feet of landfill space. Each tonne of coal fly ash used beneficially reduces the need for 1 t of virgin resources (e.g. limestone, gypsum, sand and soil) [32]. It has been successfully shown that coal fly ash can be reused in highway construction [32] and land reclamation [33]. Also, studies have been carried out to promote the recycling of coal fly ash through its zeolitization [34,35] because the major chemical composition contained in coal fly ash are SiO_2 and Al_2O_3 (60–70 and 16–20 wt.%, respectively). Synthesized zeolite materials (mixed with fly ash or in a pure form) may find its practical applications in removing heavy metals or ammonia from waste waters [34,36,37] or in gas adsorptions [38].

Although coal fly ash can be reused in the mentioned projects, the demand for re-using coal fly ash in these projects is still limited. Instead of dumping coal fly ash in landfill sites or lagoons, converting coal fly ash into mesoporous materials such as MCM-41 may provide another way for preserving the environment. In addition, compared to zeolite materials, MCM-41 material has attracted considerable attention for potential application as catalyst supports or adsorbents because of its high surface area and large pore size and volume. It is expected that the more methods of reusing coal fly ash explored, the more effort will be devoted to the disposal of coal fly ash. Presently, the use of coal fly ash as a silica source for the preparation of MCM-41 is very rare in the literature [39,40], where these studies adopted a fusion method to extract the silica source from coal fly ash. Generally, coal fly ash is treated with sodium hydroxide (1:1.2, fly ash:alkali by weight) at 550 °C for 1 h to obtain a fused mass which is cooled to room temperature and milled overnight. The obtained fused fly ash powder is mixed with water in a weight ratio of 1:4–5 and aged for 1 day at room temperature with agitation [40]. Reaction parameters used in the studies by Chang et al. [39] and Kumar et al. [40] were 110 °C for 150 h and 97 °C for 96 h, respectively. Considering the costs of equipment and energy in industrial synthesis, simple extraction of amorphous silica source from coal

fly ash with sodium hydroxide under agitation (for example, at the temperature range of 80–100 °C and duration of 2–4.5 h) is more economical than that of the fusion method.

The aim of the present study was to synthesize MCM-41 materials through a green approach by using coal fly ash as the Si source and ethyl acetate as the hydrolyser. A green synthesis approach was designed to reduce the use or generation of hazardous materials associated with the synthesis of MCM-41 while recycling of a waste material was employed. The influence of initial synthesis pH on material properties of calcined MCM-41 samples was investigated through various techniques such as XRF, XPS, XRD, FTIR, DR–UV–vis, solid state NMR, N_2 physisorption, TG-DTA, SEM and TEM. Hydrothermal stability of the calcined samples was also investigated. Removal of mixed heavy metal ions (Cr^{3+} , Cu^{2+} , Zn^{2+} , Ni^{2+} and Co^{2+}) in water by the calcined samples was evaluated.

2. Experimental

2.1. Materials

The coal fly ash used in this study was obtained from a power plant in China and was used in each experiment after a pretreatment at 120 °C for 30 min in an oven. The chemical composition of the coal fly ash was analyzed by XRF (JEOL JSX-3201Z) and is listed in Table 1. The amount of amorphous SiO_2 in the coal fly ash was 46.2 wt.% which was assayed by a quantitative X-ray diffraction (XRD) method [41]. The surface area of the coal fly ash determined by a BET surface area analyzer (Coulter SA3100) was $1.4 \text{ m}^2 \text{ g}^{-1}$. The particle size distribution of the coal fly ash was determined by a particle size analyzer (Coulter LS230). The particle size of coal fly ash ranged from 0.04 to 600 μm , with a mean diameter of 20.7 μm . Cetyltrimethylammonium bromide (CTAB, $\text{C}_{16}\text{H}_{33}(\text{CH}_3)_3\text{NBr}$, Aldrich), ethyl acetate ($\text{CH}_3\text{COOC}_2\text{H}_5$, Merck), 5.25N H_2SO_4 (BDH), NaOH pellets (Riedel-de Haen) and deionized water were used in this study.

2.2. Synthesis of MCM-41

The amorphous SiO_2 component in the coal fly ash was used as Si source for the synthesis of MCM-41. The synthesis was carried out as follows. Extraction of Si source: mixture of 30 g of fly ash and 300 ml of 2 M NaOH solution in a 1 L sealed PP bottle was kept in an oil bath at 100 °C for 4.5 h under stirred condition (300 rpm). Then the solution was separated from the mixture by a filtration process. The amounts of Si, Al and Na in the extracted solution (denoted as Si solution) were 5470, 518 and 14900 mg/l, respectively (analyzed by ICP-AES, Perkin-Elmer 3000 XL). Preparation of MCM-41 source solution: MCM-41 source solution was prepared following the procedure described in the literature [23] with modification. At 85 °C and under stirring at 300 rpm, 82 ml of the Si solution was mixed with 1 g of CTAB to obtain an aqueous solution. Then, under stirring at 600 rpm, 3.1 ml of ethyl acetate was rapidly added to the solution. After stirring the mixture for 10 min, the obtained solution was cooled down to room temperature (25 °C) by natural con-

Table 1
Elemental composition of the coal fly ash and the calcined MCM-41 samples

Sample	Synthesis pH	At. %									
		XRF (bulk)						XPS (surface)			
		Si	Al	Na	S	Ti	Fe	Si	Al	Na	Ti
Coal fly ash	n.a.	17.83	10.47	0.10	0.60	0.31	2.02	n.m.	n.m.	n.m.	n.m.
1	1.16	30.70	0	0	0	0	0	30.12	0.21	0.11	0.03
2	2.25	31.02	0.09	0.01	0	0.01	0.01	30.04	0.11	0.26	0.06
3	3.57	30.47	0.43	0.06	0	0.01	0.01	29.79	0.41	0.13	0.06
4	4.73	30.11	0.41	0.42	0.09	0.01	0.01	30.16	0.15	0.12	0.03
5	5.10	31.05	0.41	0.10	0.01	0	0.01	29.42	0.38	0.58	0.05
6	6.82	30.24	0.43	0.84	0.38	0	0.01	29.84	0.20	0.25	0.06
7	6.90	35.16	1.10	0.17	0.07	0.05	0.04	29.60	0.47	0.76	0.02
8	10.60	30.74	0.38	0	0	0.01	0.02	29.17	0.41	1.77	0.15
9	11.06	30.69	0.46	1.32	0.29	0	0.02	28.97	0.53	1.06	0.11
10	11.90	30.70	0.51	0.50	0.04	0.03	0.03	28.01	0.96	0.79	0.07

n.a.: not available, n.m.: not measured.

vection. The resultant solution was denoted as M solution in this study. Synthesis of MCM-41: 10 ml of M solution was adjusted to the selected pH by the addition of 5.25N H₂SO₄ solution under slow stirring (50 rpm). Precipitation was observed during pH adjustment. The pH adjusted solution was kept at room temperature (25 °C) for 24 h. The materials obtained were washed with deionized water and dried at 100 °C for 2 h. The dried materials were calcined under air at 550 °C for 4 h at a heating rate of 1 °C/min.

2.3. Characterization

pH values were measured with a Mettler-Toledo meter (MP 120). The bulk elemental composition of the sample was determined by a JEOL X-ray reflective fluorescence spectrometer (XRF, JSX 3201Z). The surface elemental composition of the sample was determined by X-ray photoelectron spectroscopy (XPS, Physical Electronics PHI 5600). The C 1s signal at 285 eV was utilized for making appropriate charging effect corrections. A general scan was performed to obtain the elements present in the sample. More detailed search and analysis were made for O, Si, Al, Na, S, Ti and Fe atoms. The accuracy of the absolute concentration for each element was within $\pm 10\%$. Powder X-ray diffraction (XRD) patterns of the samples were obtained using a powder diffractometer (Philips PW 1830) equipped with a Cu K α radiation. The accelerating voltage and current used were 40 kV and 20 mA, respectively. The scanning range of 2θ was set between 2 and 50°, with a step size of 0.02° and 0.01°/s. FTIR measurements were performed on a Bio-Rad FT-IR System (model: FTS 6000) using KBr self-supported pellet technique. The pellets contained about 1% of finely powdered sample and were pressed at 5 t/cm². Spectra were acquired at 2 cm⁻¹ resolution. The diffuse reflectance UV–vis spectra were measured with a Perkin-Elmer, Lambda 20 spectrophotometer. ²⁷Al MAS NMR experiments were carried out on a JEOL NM-ESH40MU solid state spectrometer at the resonance frequency of 104.3 MHz for ²⁷Al nucleus. A pulse width of 2 μ s, recycle delay time of 4 s and spinning speed of 7 kHz were used. Aluminum nitrate was employed as reference for the aluminum nucleus. Nitrogen

adsorption/desorption was carried out at 77 K using the Coulter SA3100 nitrogen physic-adsorption apparatus. The volume of adsorbed nitrogen was normalized to standard temperature and pressure (STP). Prior to the experiments, the sample was dehydrated at 150 °C for 3 h. The BET surface area was determined from the linear part of the BET plot ($p/p_0 = 0.05–0.2$). In order to study the physical aspect of the surfactant degradation within the mesopores of as-synthesized sample, thermogravimetry (TG), in combination with differential thermal analysis (DTA) (TGA/DTA, Setaram 92-18) experiments, were carried out. In these experiments, the sample was placed in a platinum holder and heated from 25 to 700 °C at a heating rate of 5 °C/min in air. Alpha alumina powder was used as a standard reference material for DTA. Surface morphology of the sample was analyzed by scanning electronic microscopy (SEM, JEOL 6300) coupled with energy dispersive X-ray analysis (EDAX). In the SEM analysis, the sample was coated with a thin layer of gold and mounted on a copper stab using a double-stick tape. TEM analysis for the samples was performed by transmission electron microscopy (TEM, JEOL 2010). The sample was suspended in methanol and transferred onto a carbon-coated (10 nm) copper grid. The sample was allowed to dry at room temperature before the TEM analysis. Hydrothermal stability of the sample was evaluated by treating the sample at 50 °C DI water (20 ml) in PP bottle for 2 weeks.

2.4. Sorption capacity of sample

All the compounds used to prepare the reagent solution were of analytic reagent grade. The mixed heavy metal ions solution containing 300 mg/l each of Cr³⁺, Cu²⁺, Zn²⁺, Ni²⁺ and Co²⁺ ions was prepared by dissolving a weighed quantity of the respective nitrate salts in deionized water. Before mixing the adsorbate with the sample, the initial pH of each solution (pH 3) was adjusted to the required value by adding 2% HNO₃. The experiments were performed at 25 \pm 0.5 °C with continuous stirring at 300 rpm. The sample (0.01 g) was left in contact with 5 ml of mixed heavy metal ions solution (300 mg/l) with an initial pH value of 3 for 240 min. It was observed that under all the exper-

imental conditions, no significant further adsorption was seen after 240 min of stirring. The sample was separated by subjecting the solution to centrifugation (5400 rpm) for over 10 min. Then, the solution was diluted and acidified with 2% HNO₃ before the ICP-AES measurement (ICP-AES, Perkin-Elmer 3000 XL). The reported values were obtained by averaging the data from two parallel experiments.

3. Results and discussion

The influence of the initial synthesis pH value on MCM-41 samples will be discussed in the following sections. This study was not intended to be an in-depth investigation of the synthesis of MCM-41 materials, but rather a demonstration of the possibility of production of MCM-41 materials from coal fly ash. Therefore, extensive analyses of the formation parameters were not provided. No attempt has been made to demonstrate the fact that the materials produced from the coal fly ash exhibit all the properties required for successful applications of mesoporous materials, which should instead belong to another phase of a more serious study.

3.1. Elemental composition

Table 1 shows the bulk and the surface composition of the coal fly ash and the calcined MCM-41 samples measured by XRF and XPS, respectively. Elements such as Al, Na, S, Ti and Fe were thought to be present as soluble oxides in the coal fly ash and were expected to form oxy-anions upon dissolution under alkaline condition during the extraction of Si source from the coal fly ash. It was shown that element S and Fe were not present on the surface of the samples (depth of surface ~ 50 Å). From SEM-EDAX analysis (picture not shown), it was found that tiny impurities were mixed with the MCM-41 samples, which was attributed to the detected sulfur element. Fig. 1 shows a clear trend of an increasing amount of elements incorporated into the

Table 2

Comparison between the bulk and the surface analysis

Sample	Synthesis pH	Bulk (XRF)			Surface (XPS)		
		Si/Al	Si/Na	Si/Ti	Si/Al	Si/Na	Si/Ti
1	1.16	n.a.	n.a.	11834	143	274	1004
2	2.25	345	2255	4293	273	116	501
3	3.57	71	471	5640	73	229	497
4	4.73	80	n.a.	5099	201	251	1005
5	5.10	73	71	4682	77	51	588
6	6.82	76	300	7427	149	119	497
7	6.90	70	36	8203	63	39	1480
8	10.60	67	23	6530	71	16	194
9	11.06	61	61	1024	55	27	263
10	11.90	32	202	705	29	36	401

n.a.: not available.

samples with synthesis pH value. This may be because most of the elements remained in the dissolved state in the synthesis solution under a low pH value. It was observed that more Al elements were incorporated into the samples at high pH values. The reason may be explained as follows. A lower degree of polycondensation of the silicate species was observed [42] when the pH value of the synthesis solution was high; thus more organic template cations compensated for the SiO⁻ groups in the samples. In addition, the TGA investigations of the Al-MCM-41 materials [2,20,43] suggested a much stronger interaction of the organic template cations with Al species than with SiO⁻ groups. As a result, more Al species were incorporated into the samples at high pH values. Furthermore, the incorporation of aluminum was generally accompanied by Na⁺ ions to balance the charge of the samples, as shown in Table 1.

Table 2 shows the comparison between the bulk and the surface mole ratio of Si/Al, Si/Na and Si/Ti of the samples. Generally, a relatively higher mole ratio of Si/Na and Si/Ti was observed in the bulk analysis. This indicated that Na and Ti elements were mainly located on the surface of the samples. For samples 1 and 2, it was shown that less Al element was incorporated into the silica framework suggesting a low interaction between the organic template with Al species at low pH values. Except samples 4 and 6, all samples showed comparative Si/Al ratios in both the bulk and the surface analysis. This observation suggested that Al was distributed equally both in the framework and on the surfaces of the samples. The reason for the phenomenon is not clear.

3.2. XRD

Table 3 presents the characteristics of MCM-41 samples synthesized from the coal fly ash. As observed in samples 1–10, the difference in the initial synthesis pH value led to different XRD data, suggesting that the initial synthesis pH played an important role in the formation of MCM-41. The hexagonal unit cell parameter, a_0 , in the calcined samples increased with synthesis pH value. This suggested that there was an increase in the amount of metal ions incorporated in the framework locations of the samples because of its (M–O; M = metal ions) longer bonding length with oxygen than Si–O [44]. A similar observation was

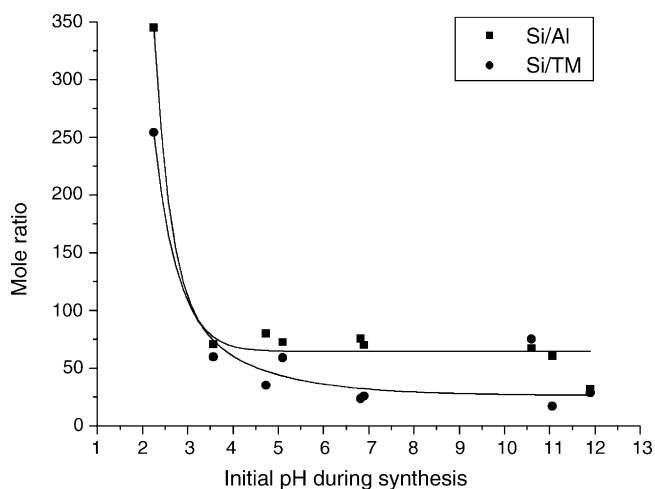


Fig. 1. Si/Al and Si/TM mole ratios of the calcined samples versus initial pH value during synthesis. TM means sum of Na, Al, Ti and Fe elements. Sample with corresponding initial pH value during preparation can be referred to in Table 1.

Table 3
Characteristics of MCM-41 samples prepared under different synthesis pH values

Sample	Synthesis pH	As-synthesized				Calcined			
		2θ (1 0 0) (°)	Intensity (counts)	d_{100} (Å)	a_0 (Å)	2θ (1 0 0) (°)	Intensity (counts)	d_{100} (Å)	a_0 (Å)
1	1.16	2.4	1250	36	42	2.8	635	31	36
2	2.25	2.6	780	34	40	2.8	635	32	36
3	3.57	2.5	1070	37	43	2.1	506	42	49
4	4.73	2.6	1652	34	40	2.7	787	32	37
5	5.10	2.6	1364	34	39	2.1	526	42	49
6	6.82	2.5	897	44	51	2.6	920	34	39
7	6.90	2.5	1279	36	41	2.6	717	33	39
8	10.60	2.3	1240	38	44	2.8	563	32	37
9	11.06	2.3	2238	38	44	2.6	787	34	40
10	11.90	2.3	1985	38	44	2.9	487	30	35

reported in the study of Zr–Mn-incorporated MCM-41 samples [45]. The hexagonal unit cell parameter, a_0 , was calculated using the formula $a_0 = 2d_{100}/\sqrt{3}$, where d_{100} was obtained from the peak in the XRD pattern by Bragg's equation ($2d \sin\theta = \lambda$, where $\lambda = 1.5406 \text{ \AA}$ for the Cu K α line). The value of a_0 was equal to the internal pore diameter plus one pore wall thickness. It should be noted that there is no regular rule in asserting incorporation of metal ions in MCM-41 as it has an amorphous structure where the bond length and the angle of metal ions on the silica surface may be changed. It was mentioned that the cation size and its coordination state play an important role in the possibility of its incorporation into the siliceous skeleton [46]. After the calcinations, the 2θ positions of all samples, except samples 3 and 5, were shifted to a higher value, which indicated a contraction of the lattice caused by template removal and subsequent condensation of the silanol groups. The observed decrease in 2θ positions of samples 3 and 5 could be caused by the difference in the silica wall thicknesses of as-synthesized and calcined samples. Since the reaction rates of hydrolysis and condensation of silicate sources are highly temperature-dependent, it can be inferred that a further condensation of silanols (residual silanol groups at the surface of the pore wall) occurred on the calcined sample during the thermal treatment to remove the template. Similar observations were reported by Zhao et al. [47] and Nishiyama et al. [48] on a study of the modification of MCM-41 by surface silylation and the preparation of MCM-48 membranes on a porous alumina support, respectively.

Fig. 2 shows the XRD patterns of the as-synthesized samples at various initial pH values. In the range of 2θ between 10 and 50° (data not shown), there was only a broad band observed which was due to the amorphous silica walls of the sample. The well defined patterns with XRD lines corresponding to {1 0 0}, {1 1 0}, {2 0 0} and {2 1 0} reflection, which are characteristics of the hexagonal lattice symmetry of the MCM-41 structure [1], could only be observed for samples 9 and 10. These XRD lines were generally taken as evidence of long range ordering of the mesostructure. However, these Bragg peaks were slightly shifted. The relatively broader and less intense main peaks of other samples (samples 1–8) indicated a distortion of the long range ordering of the mesoporous structure. The result suggests that the quality of the as-synthesized MCM-41 sample was

pH-dependent. Fig. 3 shows the XRD patterns of the calcined samples. In general, the peaks of the samples were broadened and weakened, and the deterioration of the long range ordering structure of the samples was observed. These might be due to the incorporation of metal elements into the sample causing structural irregularity supported by the FT-IR analysis shown below. Similar observations have been reported elsewhere [20,49,50]. After removal of the organic species by thermal decomposition, amorphization of sample 10 was observed. The result was probably because of a lower degree of polycondensation of the silicate species when the synthesis pH was too high, which was in agreement with the work by Voegtlin et al. [42].

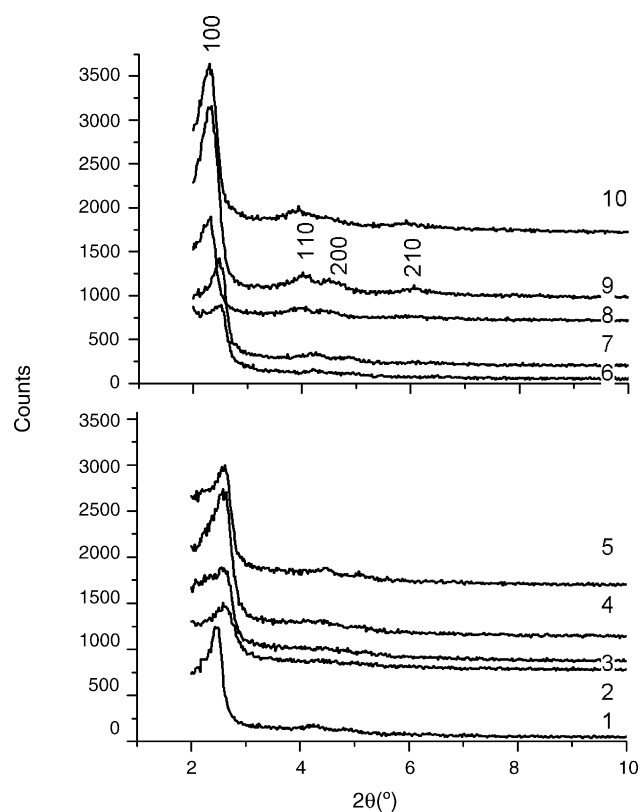


Fig. 2. Effect of initial pH value on the XRD pattern of the as-synthesized MCM-41 samples.

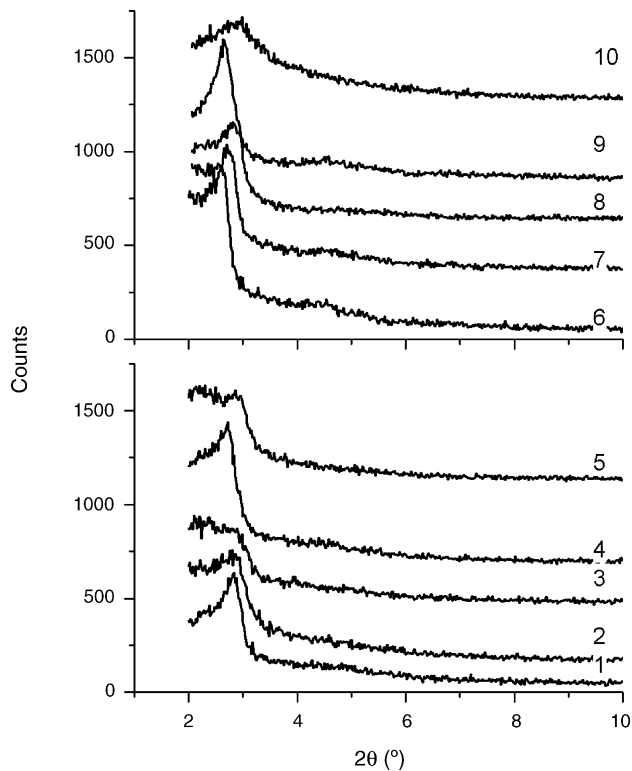


Fig. 3. Effect of initial pH value on the XRD pattern of the calcined MCM-41 samples.

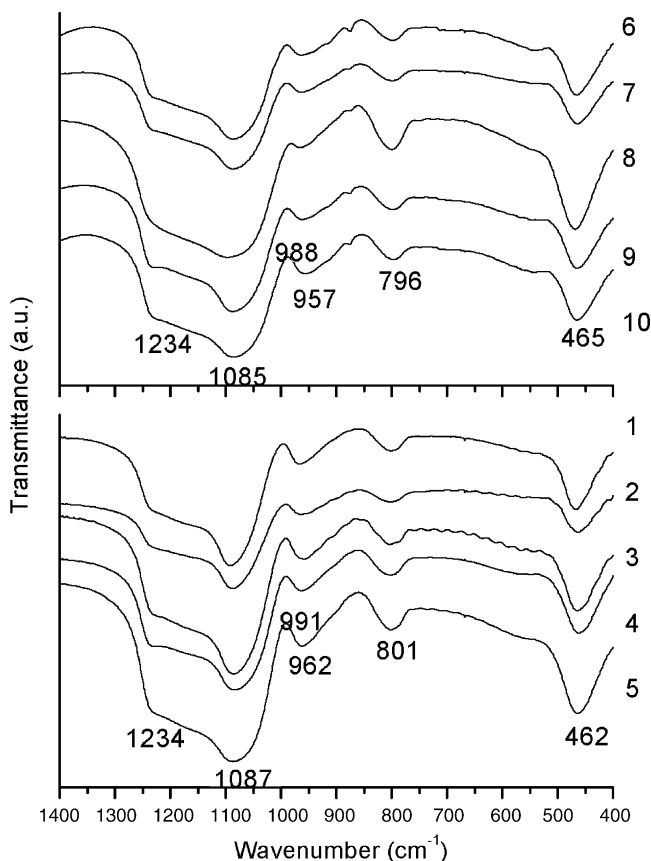


Fig. 4. FTIR spectra of the calcined samples.

3.3. Fourier transform infrared spectroscopy (FT-IR)

From the FT-IR spectra of as-synthesized samples (not shown), it exhibited absorption bands around 2921 and 2851 cm^{-1} corresponding to $n\text{-C-H}$ and $d\text{-C-H}$ vibrations of the surfactant molecules. Such bands disappeared in the calcined samples indicating the total removal of organic material during calcinations. The broad band around 3500 cm^{-1} was attributed to surface silanols and adsorbed water molecules. Moreover, the absorption bands at 1620–1650 cm^{-1} were caused by deformational vibrations of adsorbed water molecules [51]. Fig. 4 shows the FT-IR spectra of the calcined samples. Generally, for a calcined Si-MCM-41 sample, a broad band at ca. 1090 cm^{-1} and a band at ca. 810 cm^{-1} correspond to the asymmetric and symmetric Si-O stretching vibrations [52]. The bands at ca. 970 and 460 cm^{-1} were due to the stretching and bending vibrations of surface Si-O⁻ groups, respectively [53]. As the substitution of silicon by different metal ions, a shift in the lattice vibration bands to lower wave numbers was observed. The absorption band at ca. 1223 cm^{-1} was due to asymmetric stretching vibrations of the Si-O-Si bridges. Compared to Si-MCM-41, the wave number of the asymmetric Si-O-Si vibration band of the

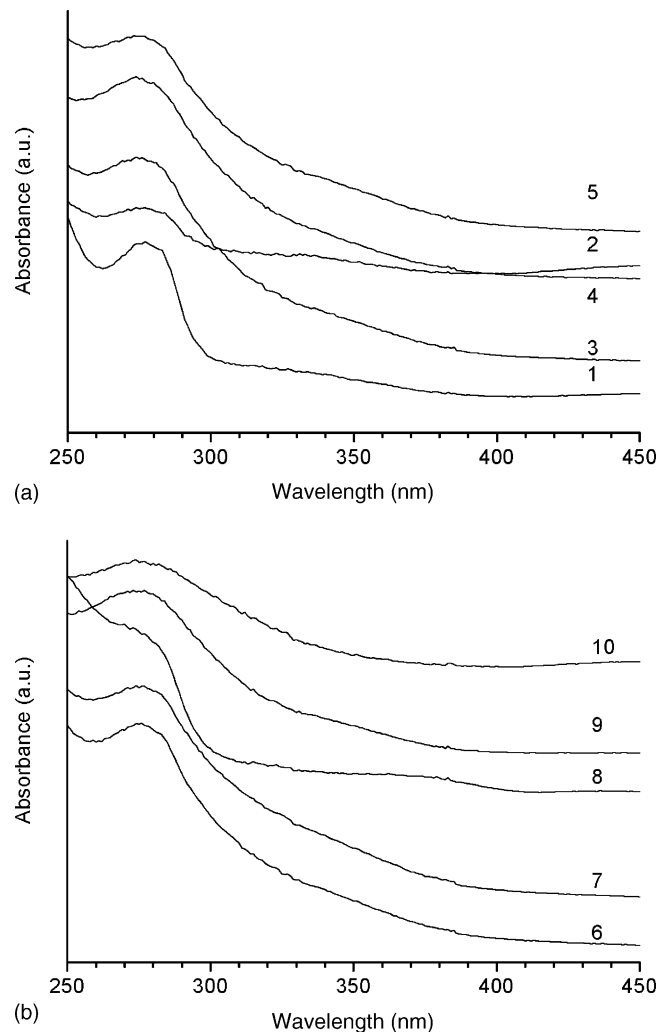


Fig. 5. Diffuse-reflectance UV-vis spectra of the calcined samples.

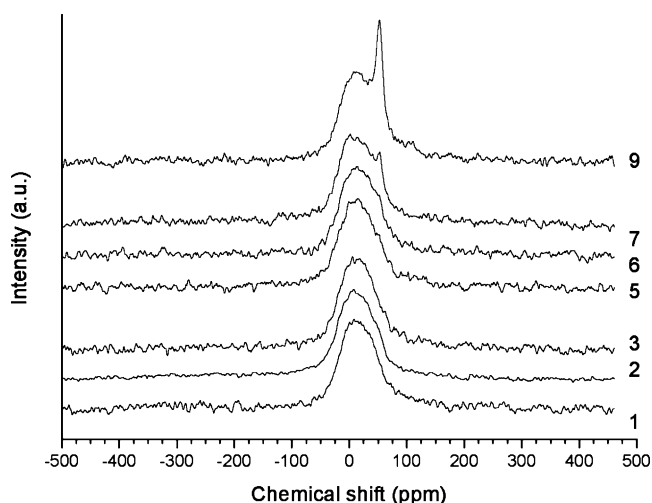


Fig. 6. ^{27}Al MAS NMR spectra of the selected calcined samples.

samples decreased to ca. 1085 cm^{-1} . The wave number of the asymmetric Si–O–M (M = metal ions) vibration bands of the samples decreased to 957 cm^{-1} . These shifts may be due to the increase in the mean Si–O distance in the walls caused by the substitution of the silicon (radius 40 pm) by the metal ions of larger size [54]. The observed shifts, which also depended on the change in the ionic radii as on the degree of substitution, were comparatively small. Therefore, only a low degree of substitution was suggested. The bands from 954 to 990 cm^{-1} were due to Si–O–M⁺ vibrations in metal-incorporated silanols [55] which was generally considered to be evidence of the incorporation of the metal ions into the framework.

3.4. Diffuse-reflectance ultraviolet–visible spectroscopy (DR–UV–vis)

DR–UV–vis analysis of the calcined samples was conducted to understand the oxidation state and environment of metal ions in the samples. Spectrum (200–1100 nm) was generally used in the DR–UV–vis analysis. However, due to the limitation of the equipment (Perkin-Elmer, Lambda 20), only wavelengths of 250–1100 nm could be used. In this case, information about Ti⁴⁺ (tetrahedral coordination) in the samples, which may be detected

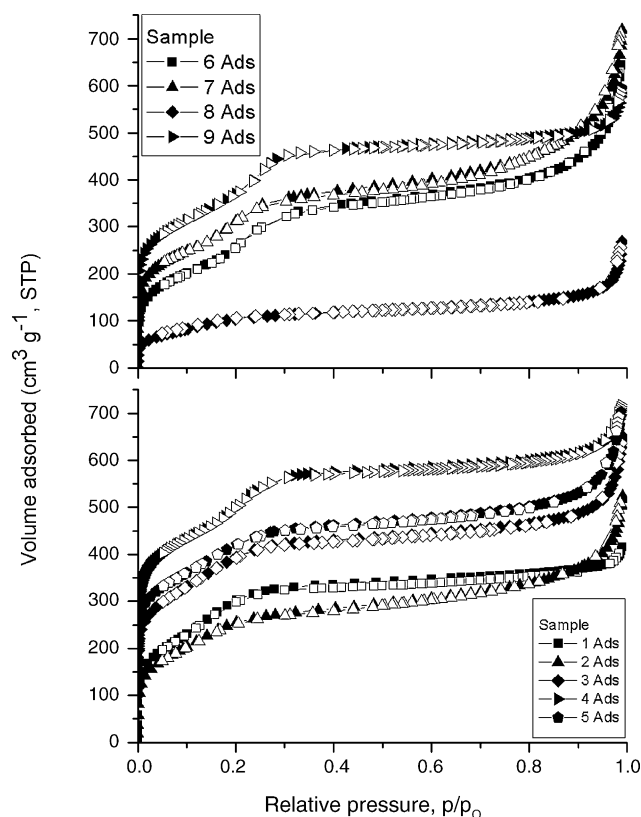


Fig. 7. N₂ adsorption/desorption isotherms of calcined samples. Filled symbols denote adsorption. Note: Samples 3, 4, 5, 7 and 9 were vertically shifted to 100, 200, 150, 50 and 100, respectively, for the sake of clarity.

using wavelengths of 210–220 nm, was unclear. Fig. 5 shows the DR–UV–vis spectra of the calcined samples. A peak around the wavelength of 273–277 nm was detected which corresponds to extra framework Ti⁴⁺ (octahedral (O_h) coordination) species [56,57]. The presence of the O_h adsorption could be the result of the water ligation to the titanium T_d species on or close to the channel surface during preparation [58]. The peak around a wavelength of 265 nm corresponding to Fe³⁺ (tetrahedral (T_d) coordination) species [55] was not clearly detected. It should be noted that UV–vis spectra provide only a rough idea of the valence state of incorporated metal ions. Detailed investigations regarding the different states and environments of metal ions on

Table 4
Textural properties of calcined MCM-41 samples prepared under different synthesis pH values

Sample	Synthesis pH	Unit cell parameter a_0 (Å)	BET surface area ($\text{m}^2\text{ g}^{-1}$)	Pore volume, V_p , ($\text{cm}^3\text{ g}^{-1}$)	Pore size ^a (Å)	Wall thickness (Å)
1	1.16	36	1149	0.6	27	9
2	2.25	36	958	0.7	29	8
3	3.57	49	1104	0.7	38	10
4	4.73	37	1086	0.7	30	8
5	5.10	49	1017	0.8	39	10
6	6.82	39	932	0.9	32	7
7	6.90	39	953	0.9	32	7
8	10.60	37	397	0.3	24	13
9	11.06	40	996	0.7	31	9
10	11.90	35	n.m.	n.m.	n.m.	n.m.

n.m.: not measured.

^a Obtained from the geometrical model with equation $W_d = cd_{100}(\rho V_p / (1 + \rho V_p))^{1/2}$, $c = 1.155$, $\rho = 2.2\text{ g cm}^{-3}$.

Table 5
Mass losses of as-synthesized MCM-41 samples prepared under different synthesis pH values

Sample	Synthesis pH	25–110 °C (%)	110–265 °C (%)	265–305 °C (%)	305–395 °C (%)	395–700 °C (%)	Total mass loss (%)
1	1.16	4.2	12.8	8.3	9.8	8.8	44.0
2	2.25	4.9	11.0	7.9	7.8	8.7	40.3
3	3.57	4.1	11.1	8.3	8.6	9.5	41.5
4	4.73	4.8	12.5	6.9	8.3	9.2	41.6
5	5.10	2.7	8.9	8.5	9.8	10.5	40.4
6	6.82	4.1	13.0	5.3	7.7	8.0	38.1
7	6.90	2.4	14.6	5.2	7.5	8.5	38.1
8	10.60	5.4	20.7	4.6	8.3	3.8	42.7
9	11.06	5.4	23.9	4.7	7.3	7.2	48.4
10	11.90	6.9	30.1	5.7	7.9	9.6	60.1
Ref. [69] ^a	n.a.	2.0	21.0	9.0	8.0	6.0	46.0

n.a.: not available.

^a Sample was synthesized by pure chemical.

the surface or in the framework of samples using techniques such as electron spin resonance (ESR) can provide better information.

3.5. ²⁷Al MAS NMR spectroscopy of the calcined samples

Solid-state NMR was used to investigate the local environment of aluminum species after calcination. Fig. 6 shows

the solid-state ²⁷Al MAS NMR spectra of the calcined samples. Peak signals at 52 ppm was due to tetrahedrally coordinated framework aluminum [59–61]; around 0 ppm was caused by distorted or octahedrally coordinated aluminum atoms at extra framework positions [59,60]. It has been reported that calcination of the as-synthesized Al-MCM-41 to remove the template led to the appearance of octahe-

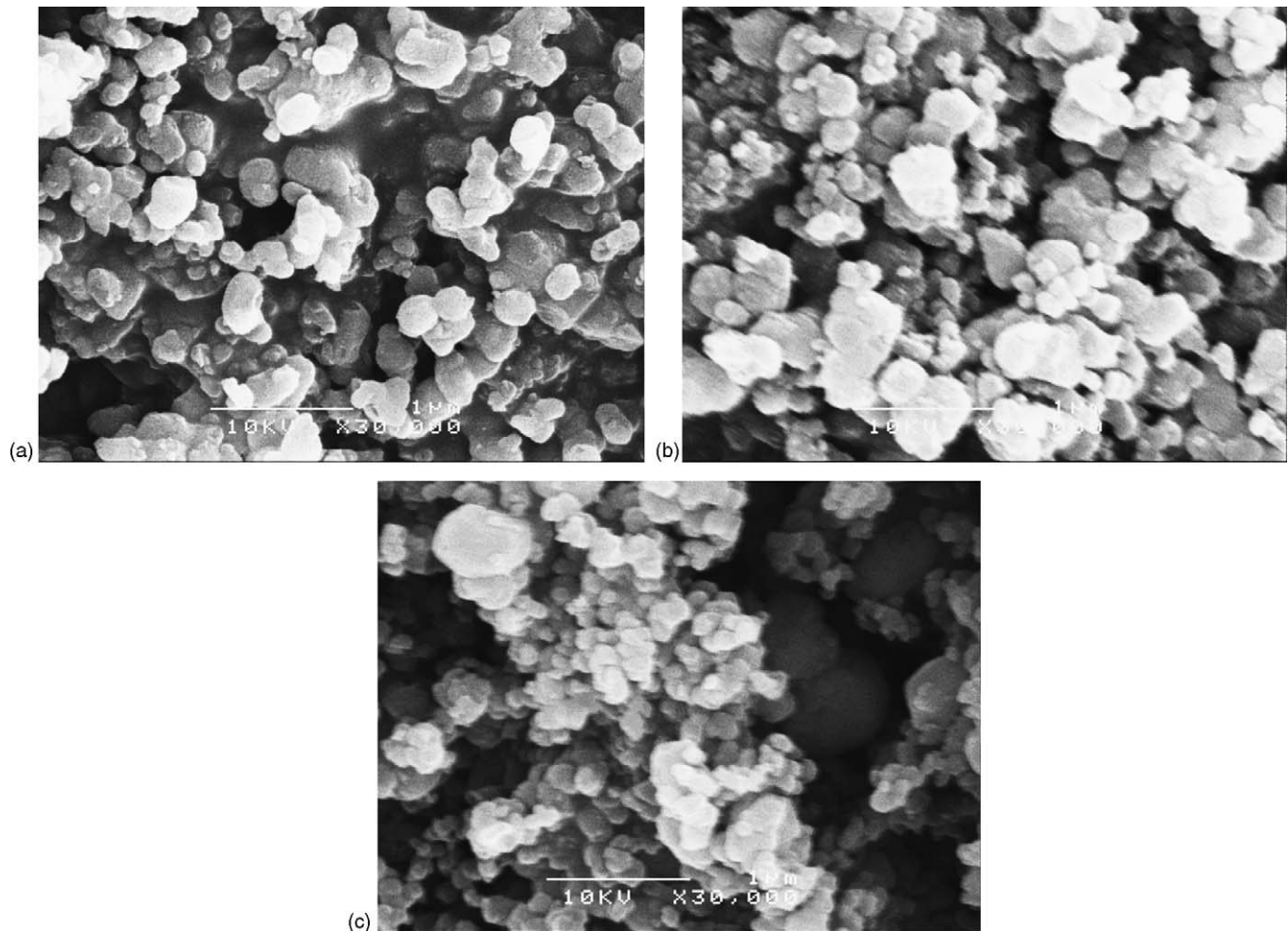


Fig. 8. SEM images of the selected samples. (a) Sample 1 (pH 1.16), (b) sample 7 (pH 6.9), (c) sample 10 (pH 11.9). (Scale bar = 1 μm).

drally coordinated extra framework aluminum species [62–64]. The intensity of 52 ppm signal increased with synthesis pH suggesting that there were more aluminum species incorporated with tetrahedral coordination in the framework under a high pH. The results provide information about the usage of these materials for acid-catalyzed reactions, in which the Bronsted acidity should be associated with the presence of tetrahedral aluminum, whereas the Lewis acidity should be associated with the presence of octahedral aluminum [65].

3.6. N_2 adsorption/desorption isotherms

The N_2 adsorption/desorption isotherms of the calcined samples are displayed in Fig. 7. Generally, all samples showed a type IV isotherm, which is a typical shape for mesoporous MCM-41. Four well-defined stages were identified as follows: (1) a gradual increase in nitrogen uptake at a low relative pressure corresponding to monolayer/multilayer adsorption on the pore walls, (2) a step at intermediate relative pressure indicating a capillary condensation within the mesopores, (3) a plateau with a slight

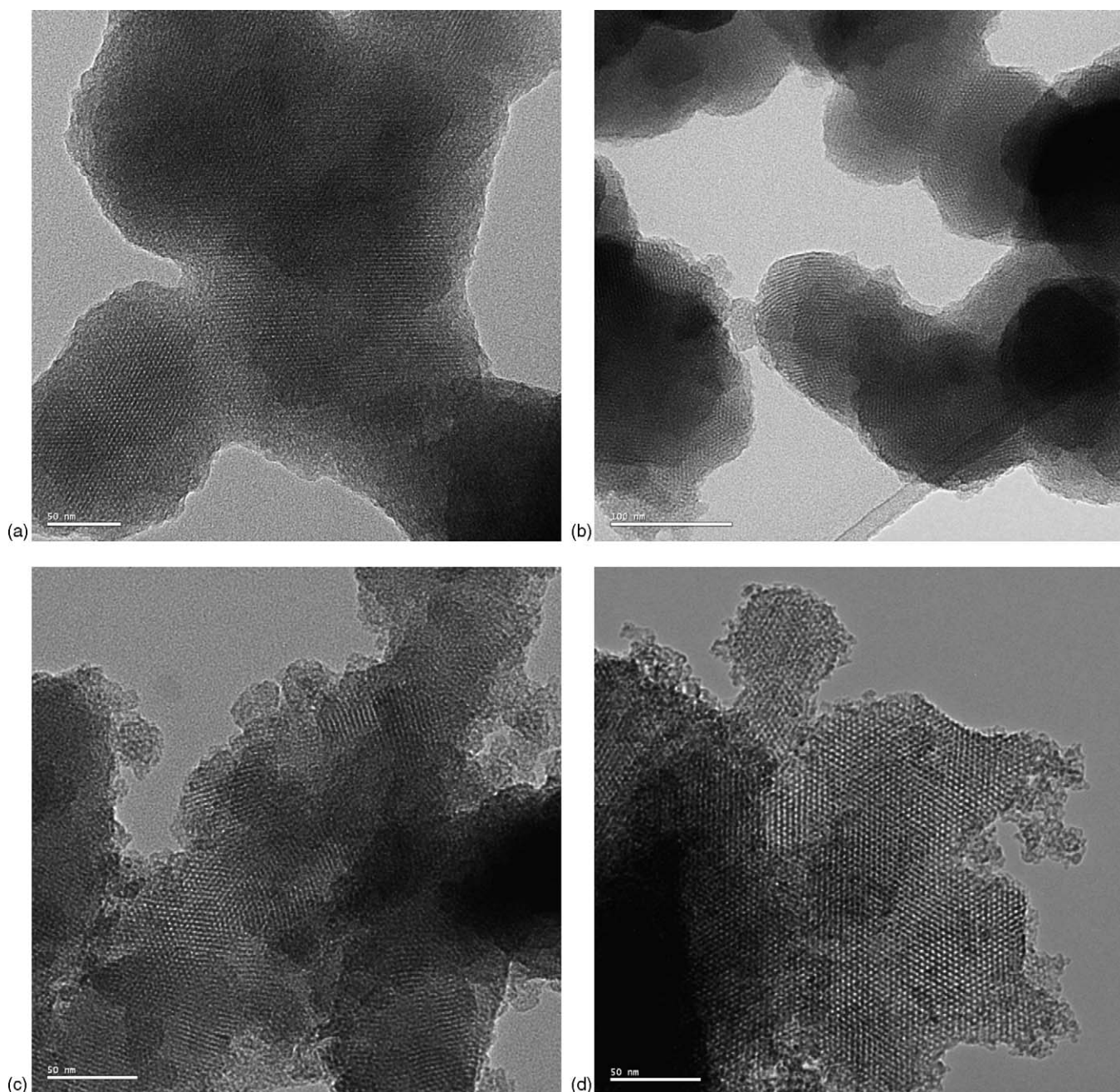


Fig. 9. TEM images of the selected calcined samples. (a) Sample 1 (scale bar: 50 nm), (b) sample 4 (scale bar: 100 nm), (c) sample 5 (scale bar: 50 nm), (d) sample 6 (scale bar: 50 nm), (e) sample 9 (scale bar: 20 nm), (f) sample 10 (scale bar: 50 nm).

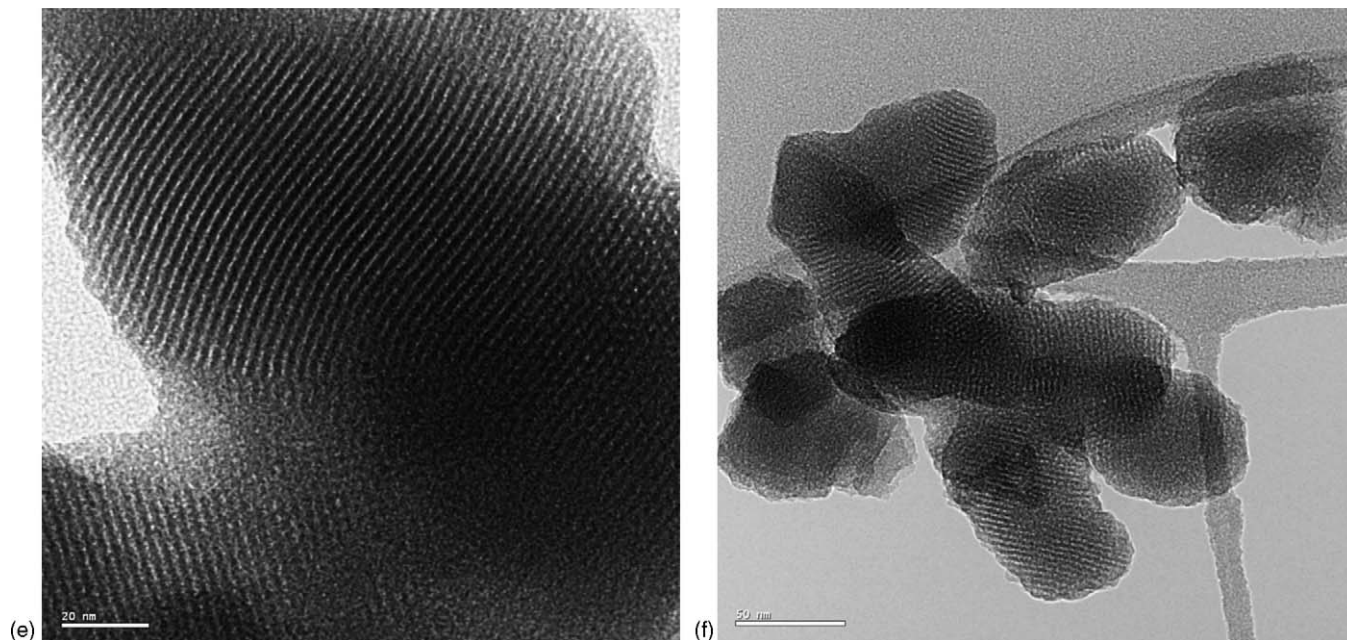


Fig. 9 (Continued).

inclination at high relative pressures associated with multilayer adsorption on the external surface of the samples [66] and (4) a sharp rise in nitrogen uptake filling all other available pores as the pressure reached saturation ($p/p_0 = 1.0$) [42]. Samples 4, 8 and 9 showed reversible type IV isotherm, which is a peculiar feature of MCM-41 materials. The near coincidence of the two branches of the isotherms could be attributed to the similar degree between the adsorption and the desorption processes. This was probably caused by the primary mesopore filling step [1,2,67]. The BET surface area, pore volume, pore size and wall thickness of the samples are shown in Table 4. The surface areas of samples lay in the range of 396.8–1148.8 m²/g. The observed low BET surface area of sample 8 was probably due to the relatively thick pore wall of the sample. Generally, the surface areas of the samples decreased with decreasing mole ratio of Si/TM. This was because the deterioration of the orderliness of the material increased with the amount of elements incorporated into the sample. However, to the best of the authors' knowledge, the BET surface areas of all samples, except sample 8, were the highest BET surface area obtained for any sample prepared from coal fly ash (735 and 842 m²/g in Chang et al. [39] and Kumar et al. [40] study, respectively).

3.7. Thermogravimetry-differential thermal analysis (TG-DTA)

Table 5 reports the mass losses of the as-synthesized samples. The as-synthesized samples had approximately 40–62% of the MCM-41 phase, whereas the remaining part corresponded to water and organic materials. From the thermal analysis, it showed that the three main processes took place upon heating of the as-synthesized samples and this was in agreement with the observations by Zhao et al. [68] and Kleitz et al. [69]. At temperatures below 150 °C, physically adsorbed water

was removed. Between 150 and 350 °C, decomposition of the organic materials happened. From 350 to 600 °C, it was often assigned to combustion of the remaining organic species, dehydroxylation and water loss associated with the condensation of the silanol groups. From Table 5, samples 8–10, which were synthesized at a higher pH value, had the highest weight loss. This may be due to the highest organic content contained in the samples. The results supported a lower degree of polycondensation of the silicate species in these samples during synthesis. Thus a larger amount of organic cations compensated for the large number of SiO⁻ groups. The results were in agreement with the works by Beck et al. [2], Kleitz et al. [69] and Cesteros et al. [20] that a higher weight loss was attributed to a higher Al content of the samples. The thermal analysis showed that the MCM-41 samples had a high thermal stability.

3.8. Scanning electron microscopy (SEM) and transmission electron microscopy (TEM)

Fig. 8 shows the selected SEM pictures of the calcined samples. It was observed that the size of particles decreased with increasing synthesis pH value. At pH 1.16, the size of particles varied between 99 and 260 nm, where the most common size was around 260 nm. The most common size of particles were around 152 and 95 nm at pH 6.9 and 11.9, respectively. In order to obtain additional information about the pore structure of the calcined samples, TEM analysis was performed, as shown in Fig. 9. The samples generally exhibited ordered hexagonal arrays of mesopores with a uniform pore size. Although some areas of the samples were not highly ordered, significant areas of the hexagonal order were observed. In parallel with the XRD data, the TEM images of sample 10 displayed distorted pore ordering, as shown in Fig. 9(f).

Table 6
Equilibrium sorption capacity and removal efficiency of mixed metal ions by selected MCM-41 samples

Initial conc. (mg/l)	Samples	Equilibrium sorption capacity ^a (removal efficiency %) ^b					Equilibrium pH (selectivity sequence)
		Co ²⁺	Cr ³⁺	Cu ²⁺	Ni ²⁺	Zn ²⁺	
300	4	1.92 (0.98)	4.49 (2.33)	3.21 (1.59)	1.28 (0.64)	7.69 (4.00)	2.75 (Zn ²⁺ > Cr ³⁺ > Cu ²⁺ > Co ²⁺ > Ni ⁺)
	7	9.65 (3.58)	12.28 (4.67)	13.16 (4.76)	7.89 (2.87)	14.91 (5.67)	2.76 (Zn ²⁺ > Cu ²⁺ > Cr ³⁺ > Co ²⁺ > Ni ⁺)
	9	5.49 (2.29)	7.13 (3.04)	0.70 (0.28)	3.86 (1.57)	7.91 (3.38)	2.82 (Zn ²⁺ > Cr ³⁺ > Co ²⁺ > Ni ⁺ > Cu ²⁺)

^a Equilibrium sorption capacity was evaluated as $q_e = (C_0 - C_e)/m \times V$, where C_0 is the initial metal ions concentration (mg/l), C_e is the equilibrium metal ions concentration (mg/l), V is the volume of the aqueous phase (l), and m is the amount of the sample used (g). Unit of equilibrium sorption capacity is mg/g.

^b Removal efficiency was evaluated as $(C_0 - C_e)/C_0 \times 100$. (T , 25 °C; stirring speed, 300 rpm; time, 240 min; pH, 3; V , 5 ml; m , 0.01 g).

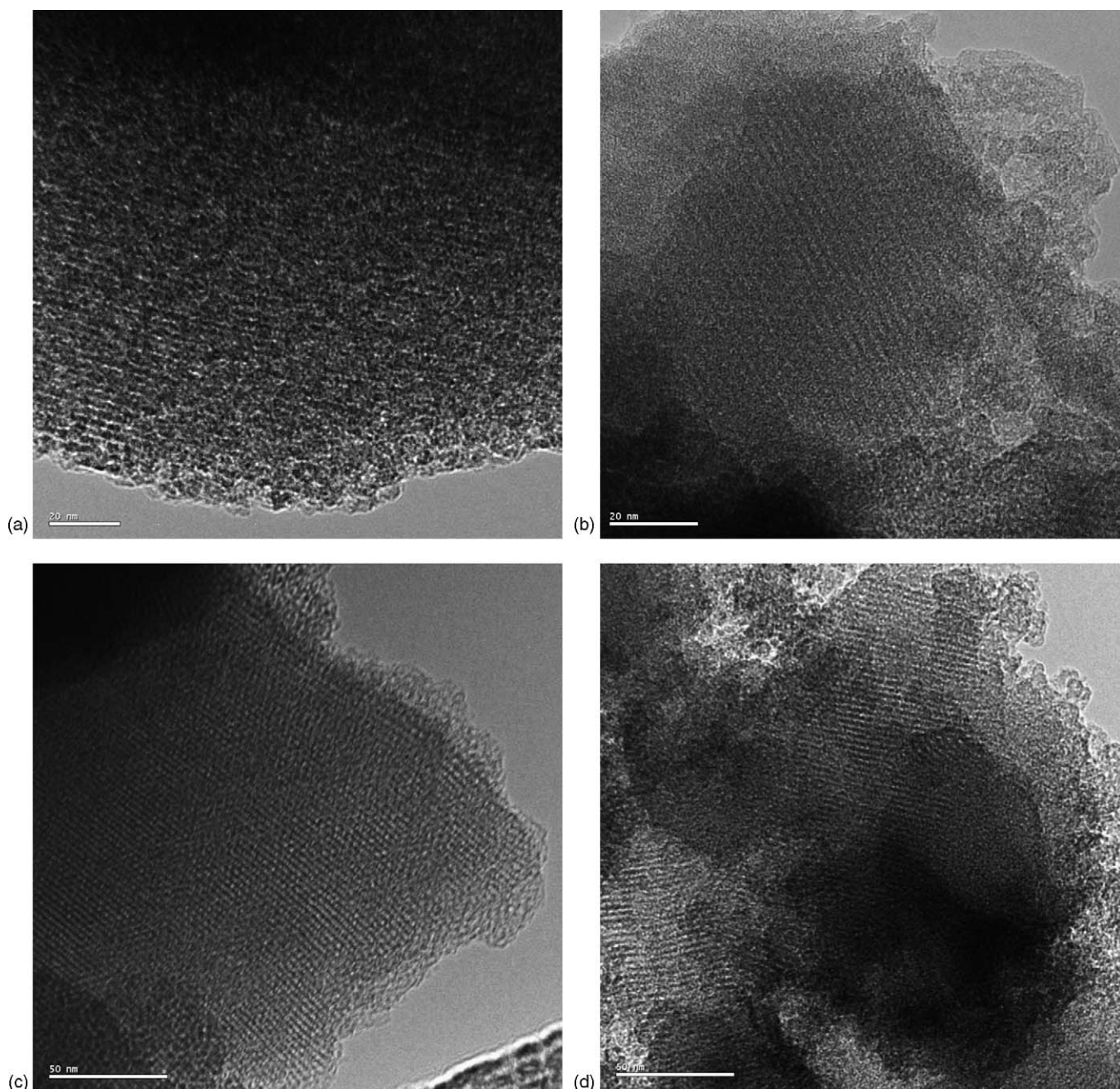


Fig. 10. TEM images of the hydrothermal treated samples (50 °C for 2 weeks). (a) Sample 1 (scale bar: 20 nm), (b) sample 2 (scale bar: 20 nm), (c) sample 4 (scale bar: 50 nm), (d) sample 6 (scale bar: 50 nm), (e) sample 7 (scale bar: 50 nm), (f) sample 9 (scale bar: 20 nm).

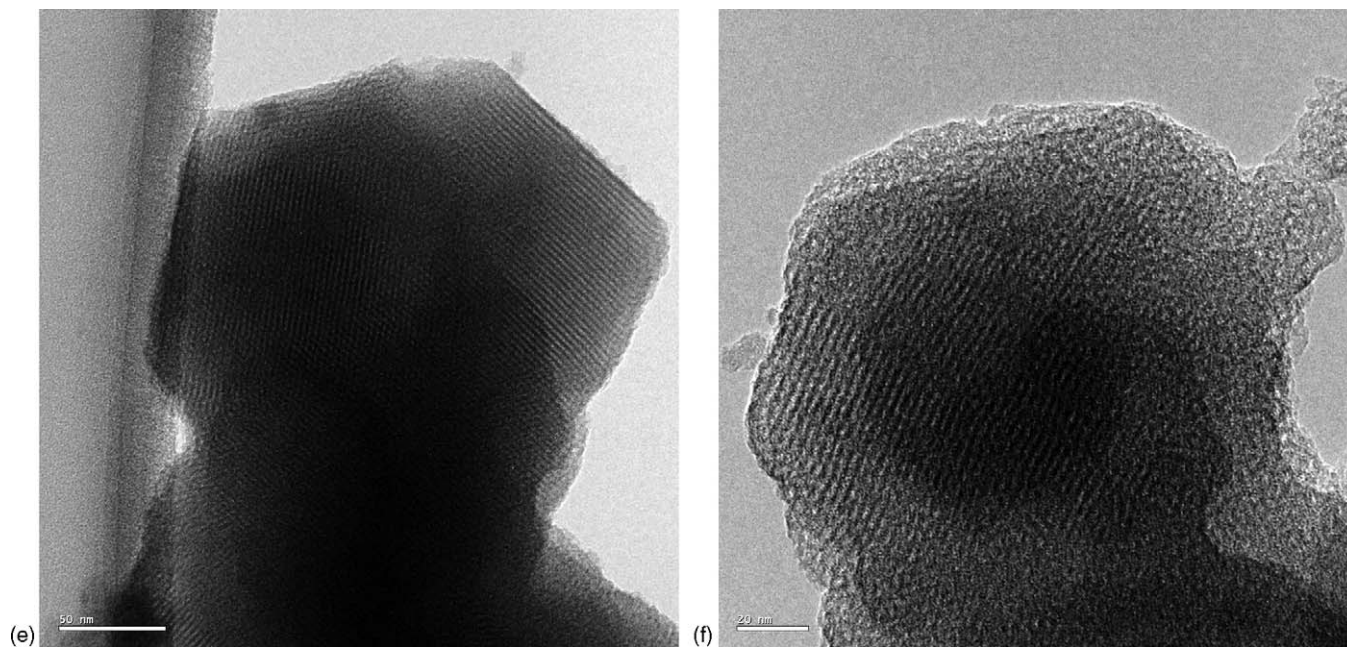


Fig. 10 (Continued).

3.9. Hydrothermal stability and removal of mixed heavy metal ions by synthesized MCM-41 samples

The yielding of the calcined MCM-41 samples was about 20–25%. Yielding was calculated as: (weight of calcined MCM-41 produced)/(weight of reactive species used in the synthesis: coal fly ash, NaOH pellets, CTAB and ethyl acetate) \times 100. It is worth noting that the proposed synthesis method was far simpler and less time-consuming than those reported in the literature [39,40]. After the conversion process (synthesis of MCM-41 materials from the coal fly ash), the residual ash was also converted into adsorbent for the treatment of wastewater containing mixed heavy metal ions (Co^{2+} , Cr^{3+} , Cu^{2+} , Zn^{2+} and Ni^{2+}) [37]. It was shown that thorough reuse of the coal fly ash is possible.

Fig. 10 shows the TEM images of selected samples which were taken after they have been treated in DI water at 50 °C for 2 weeks. It was observed that the samples synthesized at high pH values were more hydrothermally stable than those at low pH values. The pore structure of these high pH samples were in a relative good shape. This may be due to the presence of more incorporated metal ions of the samples, creating a negative charge on the surface of the pore walls, which repel OH^- ions and prevent the hydrolysis of siloxane bonds. Table 6 lists the equilibrium sorption capacity and the removal efficiency of metal ions by the selected samples. The results show that the sample synthesized around neutral pH had the highest removal efficiency and equilibrium sorption capacity of the metal ions at the tested conditions. Also, the selectivity sequence of metal ions was different among samples. The observed differences may be due to the different nature and surface chemistry of the sample which was synthesized under a specified pH and the particle size of sample. The results showed that the calcined MCM-41 samples (without any functional organic groups grafted onto the surface of the sample) are poor adsorbents for the removal of

mixed heavy metal ions. However, studies have shown that the sorption capacity of metal ions by calcined MCM-41 samples can be significantly improved through post-modification of the MCM-41 samples to improve its affinity to metal ions [70–74]. The synthesized MCM-41 materials possessed a large pore size, pore volume, BET surface area and good hydrothermal stability. These properties enabled them to accommodate a larger concentration of functional groups on their surface. It has been shown that the sorption capacity of metal ions increases with increasing concentration of the grafted functional group [75]. It is expected that the calcined MCM-41 samples can be used as an adsorbent in the treatment of waste water after grafting functional organic groups (such as thiol or amine) onto its surface.

4. Conclusions

Based on the experimental study, it was concluded that pure (free of coal fly ash) and ordered MCM-41 materials could be successfully synthesized from coal fly ash at room temperature during 24 h of reaction. The yielding of the calcined MCM-41 samples was about 20–25%. The impurities in the coal fly ash are not detrimental to the formation of MCM-41 at the tested conditions; however, traces of elements such as Al, Na, Ti and Fe were inevitably incorporated into the synthesized materials. The incorporation of aluminum species into the framework of MCM-41 makes the samples exhibit moderate acidity, which is useful for application in catalysis and adsorption. The results show that material properties of the calcined sample are dependent on the initial synthesis pH. It was shown that the synthesized MCM-41 materials possessed large pore size, pore volume and BET surface area. The high thermal and hydrothermal stability enabled them to be good candidates for application as catalysts or adsorbents after the proper post-processing is conducted. The synthesized MCM-41 materials can be used as ‘starting materi-

als' where post-modification of the materials is needed so that specific usages of the materials can be applied. For example, through post-modification of the surface property of the calcined MCM-41 materials, the synthesized MCM-41 materials may find application in the treatment of waste water. This study demonstrates that converting coal fly ash into mesoporous materials not only eliminates the disposal problem of coal fly ash but also turns a waste material into a useful one. The proposed method provides another way of recycling coal fly ash.

Acknowledgements

The authors would like to thank Ching-Yin Lo for his help on parts of the synthesis of MCM-41. Technical support from the Materials Characterization and Preparation Facility, Advanced Engineering Materials Facility, Department of Chemical Engineering of the Hong Kong University of Science and Technology are gratefully acknowledged. Funding for this research was provided by RGC Grant HKUST 6188/03E and 6132/04E.

References

- [1] C.T. Kresge, M.E. Leonowicz, W.J. Roth, J.C. Vartuli, J.S. Beck, Ordered mesoporous molecular-sieves synthesized by a liquid-crystal template mechanism, *Nature* 359 (1992) 710–712.
- [2] J.S. Beck, J.C. Vartuli, W.J. Roth, M.E. Leonowicz, C.T. Kresge, K.D. Schmitt, C.T.W. Chu, D.H. Olson, E.W. Sheppard, S.B. McCullen, J.B. Higgins, J.L. Schlenker, A new family of mesoporous molecular-sieves prepared with liquid-crystal templates, *J. Am. Chem. Soc.* 114 (1992) 10834–10843.
- [3] J.S. Beck, J.C. Vartuli, Recent advances in the synthesis, characterization and applications of mesoporous molecular sieves, *Curr. Opin. Solid State Mater. Sci.* 1 (1996) 76–87.
- [4] X.S. Zhao, G.Q.M. Lu, G.J. Millar, Advances in mesoporous molecular sieve MCM-41, *Ind. Eng. Chem. Res.* 35 (1996) 2075–2090.
- [5] P. Selvam, S.K. Bhatia, C.G. Sonwane, Recent advances in processing and characterization of periodic mesoporous MCM-41 silicate molecular sieves, *Ind. Eng. Chem. Res.* 40 (2001) 3237–3261.
- [6] N. Yao, G.X. Xiong, K.L. Yeung, S.S. Sheng, M.Y. He, W.S. Yang, X.M. Liu, X.H. Bao, Ultrasonic synthesis of silica-alumina nanomaterials with controlled mesopore distribution without using surfactants, *Langmuir* 18 (2002) 4111–4117.
- [7] S. Biz, M.L. Occelli, Synthesis and characterization of mesostructured materials, *Catal. Rev. Sci. Eng.* 40 (1998) 329–407.
- [8] T. Kimura, Surfactant-templated mesoporous aluminophosphate-based materials and the recent progress, *Micropor. Mesopor. Mater.* 77 (2005) 97–107.
- [9] A. Corma, From microporous to mesoporous molecular sieve materials and their use in catalysis, *Chem. Rev.* 97 (1997) 2373–2419.
- [10] N. Schmidt, M. Stocker, E. Hansen, D. Kporiaye, O.H. Ellestad, MCM-41—a model system for adsorption studies on mesoporous materials, *Micropor. Mater.* 3 (1995) 443–448.
- [11] L. Mercier, T.J. Pinnavaia, Access in mesoporous materials: Advantages of a uniform pore structure in the design of a heavy metal ion adsorbent for environmental remediation, *Adv. Mater.* 9 (1997) 500–503.
- [12] L. Mercier, T.J. Pinnavaia, Heavy metal ion adsorbents formed by the grafting of a thiol functionality to mesoporous silica molecular sieves: Factors affecting Hg(II) uptake, *Environ. Sci. Technol.* 32 (1998) 2749–2754.
- [13] K.Y. Ho, G. McKay, K.L. Yeung, Selective adsorbents from ordered mesoporous silica, *Langmuir* 19 (2003) 3019–3024.
- [14] J.F. Diaz, K.J. Balkus, Enzyme immobilization in MCM-41 molecular sieve, *J. Mol. Catal. B Enz.* 2 (1996) 115–126.
- [15] M. Grun, A.A. Kurganov, S. Schacht, F. Schuth, K.K. Unger, Comparison of an ordered mesoporous aluminosilicate, silica, alumina, titania and zirconia in normal-phase high-performance liquid chromatography, *J. Chromatogr. A* 740 (1996) 1–9.
- [16] A. Corma, Preparation and catalytic properties of new mesoporous materials, *Top. Catal.* 4 (1997) 249–260.
- [17] S. Morin, P. Ayrault, S. ElMouahid, N.S. Gnep, M. Guisnet, Particular selectivity of m-xylene isomerization over MCM-41 mesoporous aluminosilicates, *Appl. Catal. A Gen.* 159 (1997) 317–331.
- [18] M.J. Climent, A. Corma, R. Guil-Lopez, S. Iborra, J. Primo, Use of mesoporous MCM-41 aluminosilicates as catalysts in the preparation of fine chemicals—a new route for the preparation of Jasminaldehyde with high selectivity, *J. Catal.* 175 (1998) 70–79.
- [19] K.R. Kloetstra, M. vanLaren, H. vanBekum, Binary caesium lanthanum oxide supported on MCM-41: a new stable heterogeneous basic catalyst, *J. Chem. Soc. Faraday Trans.* 93 (1997) 1211–1220.
- [20] Y. Cesteros, G.L. Haller, Several factors affecting Al-MCM41 synthesis, *Micropor. Mesopor. Mater.* 43 (2001) 171–179.
- [21] G.A. Eimer, L.B. Pierella, G.A. Monti, O.A. Anunziata, Synthesis and characterization of Al-MCM-41 and Al-MCM-48 mesoporous materials, *Catal. Lett.* 78 (2002) 65–75.
- [22] N. Kumar, V. Nieminen, L.E. Lindfors, T. Salmi, D.Y. Murzin, E. Laine, T. Heikkila, Cu-H-MCM-41, H-MCM-41 and Na-MCM-41 mesoporous molecular sieve catalysts for isomerization of 1-butene to isobutene, *Catal. Lett.* 78 (2002) 105–110.
- [23] W.L. Dai, H. Chen, Y. Cao, H.X. Li, S.H. Xie, K.N. Fan, Novel economic and green approach to the synthesis of highly active W-MCM41 catalyst in oxidative cleavage of cyclopentene, *Chem. Commun.* (2003) 892–893.
- [24] S.A. Bagshaw, F. Testa, Wairakei geothermal silica, a low cost reagent for the synthesis of mesostructured M41S aluminosilicate molecular sieves, *Micropor. Mesopor. Mater.* 39 (2000) 67–75.
- [25] G. Belardi, S. Massimilla, L. Piga, Crystallization of K–L and K–W zeolites from fly ash, *Resour. Conserv. Recycl.* 24 (1998) 167–181.
- [26] G. Ferraiolo, M. Zilli, A. Converti, Fly-ash disposal and utilization, *J. Chem. Technol. Biotechnol.* 47 (1990) 281–305.
- [27] C.L. Carlson, D.C. Adriano, Environmental impacts of coal combustion residues, *J. Environ. Qual.* 22 (1993) 227–247.
- [28] R. Kikuchi, Application of coal ash to environmental improvement—transformation into zeolite, potassium fertilizer, and FGD absorbent, *Resour. Conserv. Recycl.* 27 (1999) 333–346.
- [29] C. Zevenbergen, J.P. Bradley, L.P. Van Rееuwijk, A.K. Shyam, O. Hjelm, R.N.J. Comans, Clay formation and metal fixation during weathering of coal fly ash, *Environ. Sci. Technol.* 33 (1999) 3405–3409.
- [30] M. Park, C.L. Choi, W.T. Lim, M.C. Kim, J. Choi, N.H. Heo, Molten-salt method for the synthesis of zeolitic materials. I. Zeolite formation in alkaline molten-salt system, *Micropor. Mesopor. Mater.* 37 (2000) 81–89.
- [31] K.S. Hui, C.Y.H. Chao, Pure, single phase, chamfered-edge zeolite 4A synthesized from coal fly ash as a builder in detergents, *J. Hazard. Mater.* 137 (2006) 401–409.
- [32] U.S. Environmental Protection Agency, Using coal fly ash in highway construction: a guide to benefits and impacts, EPA-530-K-05-002, April 2005.
- [33] Land uses of coal fly ash-benefits and barriers, <http://www.iea-coal.org.uk>.
- [34] X. Querol, N. Moreno, J.C. Umana, A. Alastuey, E. Hernandez, A. Lopez-Soler, F. Plana, Synthesis of zeolites from coal fly ash: an overview, *Int. J. Coal Geol.* 50 (2002) 413–423.
- [35] K.S. Hui, C.Y.H. Chao, Effects of step-change of synthesis temperature on synthesis of zeolite 4A from coal fly ash, *Micropor. Mesopor. Mater.* 88 (2006) 145–151.
- [36] G.G. Hollman, G. Steenbruggen, M. Janssen-Jurkovicova, A two-step process for the synthesis of zeolites from coal fly ash, *Fuel* 78 (1999) 1225–1230.
- [37] K.S. Hui, C.Y.H. Chao, S.C. Kot, Removal of mixed heavy metal ions in waste water by zeolite 4A and residual products from recycled coal fly ash, *J. Hazard. Mater.* 127 (2005) 89–101.
- [38] A. Srinivasan, M.W. Grutzeck, The adsorption of SO₂ by zeolites synthesized from fly ash, *Environ. Sci. Technol.* 33 (1999) 1464–1469.
- [39] H.L. Chang, C.M. Chun, I.A. Aksay, W.H. Shih, Conversion of fly ash into mesoporous aluminosilicate, *Ind. Eng. Chem. Res.* 38 (1999) 973–977.

- [40] P. Kumar, N. Mal, Y. Oumi, K. Yamana, T. Sano, Mesoporous materials prepared using coal fly ash as the silicon and aluminium source, *J. Mater. Chem.* 11 (2001) 3285–3290.
- [41] S.C. White, E.D. Case, Characterization of fly-ash from coal-fired power-plants, *J. Mater. Sci.* 25 (1990) 5215–5219.
- [42] A.C. Voegtlin, A. Matijasic, J. Patarin, C. Sauerland, Y. Grillet, L. Huve, Room-temperature synthesis of silicate mesoporous MCM-41-type materials: Influence of the synthesis pH on the porosity of the materials obtained, *Micropor. Mater.* 10 (1997) 137–147.
- [43] R. Schmidt, D. Akporiaye, M. Stocker, O.H. Ellestad, in: J. Weitkamp, H.G. Karge, H. Pfeifer, W. Holderich (Eds.), *Zeolites and related microporous materials: State of the art 1994*, Elsevier, Amsterdam, 1994, p. 61.
- [44] M.J. Sienko, R.A. Plane, *Chemistry Principles and Applications*, 1st ed., McGraw-Hill, New York, 1979.
- [45] M. Selvaraj, P.K. Sinha, K. Lee, I. Ahn, A. Pandurangan, T.G. Lee, Synthesis and characterization of Mn-MCM-41 and Zr-Mn-MCM-41, *Micropor. Mesopor. Mater.* 78 (2005) 139–149.
- [46] J.Y. Ying, C.P. Mehnert, M.S. Wong, Synthesis and applications of supramolecular-templated mesoporous materials, *Angew. Chem. Int. Ed.* 38 (1999) 56–77.
- [47] X.S. Zhao, G.Q. Lu, Modification of MCM-41 by surface silylation with trimethylchlorosilane and adsorption study, *J. Phys. Chem. B* 102 (1998) 1556–1561.
- [48] N. Nishiyama, D.H. Park, Y. Egashira, K. Ueyama, Pore size distributions of silylated mesoporous silica MCM-48 membranes, *Sep. Purif. Technol.* 32 (2003) 127–132.
- [49] J. Rathousky, A. Zukal, O. Franke, G. Schulzekloff, Adsorption on MCM-41 mesoporous molecular-sieves. 1. Nitrogen isotherms and parameters of the porous structure, *J. Chem. Soc. Faraday Trans.* 90 (1994) 2821–2826.
- [50] Z.H. Luan, H.Y. He, W.Z. Zhou, C.F. Cheng, J. Klinowski, Effect of structural aluminum on the mesoporous structure of MCM-41, *J. Chem. Soc. Faraday Trans.* 91 (1995) 2955–2959.
- [51] A.V. Kiselev, V.I. Lygin, *Infrared Spectra of Surface Compounds and Adsorbed Substances*, 1st ed., Nauka, Moscow, 1992.
- [52] A.A. Romero, M.D. Alba, W.Z. Zhou, J. Klinowski, Synthesis and characterization of the mesoporous silicate molecular sieve MCM-48, *J. Phys. Chem. B* 101 (1997) 5294–5300.
- [53] R. Takahashi, S. Sato, T. Sodesawa, M. Kawakita, K. Ogura, High surface-area silica with controlled pore size prepared from nanocomposite of silica and citric acid, *J. Phys. Chem. B* 104 (2000) 12184–12191.
- [54] R.D. Shannon, C.T. Prewitt, Revised values of effective ionic radii, *Acta Cryst. B* 26 (1970) 1046–1048.
- [55] M. Selvaraj, B.H. Kim, T.G. Lee, FTIR studies on selected mesoporous metallosilicate molecular sieves, *Chem. Lett.* 34 (2005) 1290–1291.
- [56] K.A. Koyano, T. Tatsumi, Synthesis of titanium-containing mesoporous molecular sieves with a cubic structure, *Chem. Commun.* (1996) 145–146.
- [57] M.S. Morey, S. O'Brien, S. Schwarz, G.D. Stucky, Hydrothermal and postsynthesis surface modification of cubic, MCM-48, and ultralarge pore SBA-15 mesoporous silica with titanium, *Chem. Mater.* 12 (2000) 898–911.
- [58] M.C. Chao, H.P. Lin, C.Y. Mou, B.W. Cheng, C.F. Cheng, Synthesis of nano-sized mesoporous silicas with metal incorporation, *Catal. Today* 97 (2004) 81–87.
- [59] C.Y. Chen, H.X. Li, M.E. Davis, Studies on mesoporous materials. I. Synthesis and characterization of MCM-41, *Micropor. Mater.* 2 (1993) 17–26.
- [60] R.B. Borade, A. Clearfield, Synthesis of aluminum-rich MCM-41, *Catal. Lett.* 31 (1995) 267–272.
- [61] Z.H. Luan, C.F. Cheng, W.Z. Zhou, J. Klinowski, Mesopore molecular sieve MCM-41 containing framework aluminum, *J. Phys. Chem.* 99 (1995) 1018–1024.
- [62] B. Chakraborty, B. Viswanathan, Surface acidity of MCM-41 by in situ IR studies of pyridine adsorption, *Catal. Today* 49 (1999) 253–260.
- [63] A. Matsumoto, H. Chen, K. Tsutsumi, M. Grun, K. Unger, Novel route in the synthesis of MCM-41 containing framework aluminum and its characterization, *Micropor. Mesopor. Mat.* 32 (1999) 55–62.
- [64] H. Kosslick, G. Lischke, G. Walther, W. Storek, A. Martin, R. Fricke, Physico-chemical and catalytic properties of Al-, Ga- and Fe-substituted mesoporous materials related to MCM-41, *Micropor. Mater.* 9 (1997) 13–33.
- [65] M. Selvaraj, A. Pandurangan, P.K. Sinha, Comparison of mesoporous Zn–Al-MCM-41 and Al-MCM-41 molecular sieves in the production of *p*-cymene by isopropylation of toluene, *Ind. Eng. Chem. Res.* 43 (2004) 2399–2412.
- [66] S.J. Gregg, K.S.W. Sing, *Adsorption Surface Area and Porosity*, 1st ed., Academic Press, London, 1967.
- [67] P.J. Branton, P.G. Hall, K.S.W. Sing, Physisorption of nitrogen and oxygen by MCM-41, A model mesoporous adsorbent, *J. Chem. Soc. Chem. Commun.* (1993) 1257–1258.
- [68] X.S. Zhao, G.Q. Lu, A.K. Whittaker, G.J. Millar, H.Y. Zhu, Comprehensive study of surface chemistry of MCM-41 using Si-29 CP/MAS NMR, FTIR, pyridine-TPD, and TGA, *J. Phys. Chem. B* 101 (1997) 6525–6531.
- [69] F. Kleitz, W. Schmidt, F. Schuth, Calcination behavior of different surfactant-templated mesostructured silica materials, *Micropor. Mesopor. Mater.* 65 (2003) 1–29.
- [70] X. Feng, G.E. Fryxell, L.Q. Wang, A.Y. Kim, J. Liu, K.M. Kemner, Functionalized monolayers on ordered mesoporous supports, *Science* 276 (1997) 923–926.
- [71] J. Liu, X.D. Feng, G.E. Fryxell, L.Q. Wang, A.Y. Kim, M. Gong, Hybrid mesoporous materials with functionalized monolayers, *Chem. Eng. Technol.* 21 (1998) 97–100.
- [72] L. Bois, A. Bonhomme, A. Ribes, B. Pais, G. Raffin, F. Tessier, Functionalized silica for heavy metal ions adsorption, *Colloid Surf. A Physicochem. Eng. Asp.* 221 (2003) 221–230.
- [73] Y. Kim, B. Lee, J. Yi, Preparation of functionalized mesostructured silica containing magnetite (MSM) for the removal of copper ions in aqueous solutions and its magnetic separation, *Sep. Sci. Technol.* 38 (2003) 2533–2548.
- [74] H. Lee, J.H. Yi, Removal of copper ions using functionalized mesoporous silica in aqueous solution, *Sep. Sci. Technol.* 36 (2001) 2433–2448.
- [75] Y. Kim, J. Yi, Advances in environmental technologies via the application of mesoporous materials, *J. Ind. Eng. Chem.* 10 (2004) 41–51.